Thermal Science and Engineering Progress 18 (2020) 100515

Contents lists available at ScienceDirect

Thermal Science and Engineering Progress

journal homepage: www.elsevier.com/locate/tsep

Novel fan configuration for distributed propulsion systems with boundary layer ingestion on an hybrid wing body airframe

Esteban Valencia[a,*], Victor Alulema[a], Dario Rodriguez[a], Panagiotis Laskaridis[b], Ioannis Roumeliotis[b]

[a] Department or Mechanical Engineering, Escuela Politecnica Nacional, Quito, Pichincha 170517, Ecuador
[b] Centre for Propulsion Engineering, Cranfield University, United Kingdom

ARTICLE INFO

Keywords:
Turboelectric distributed propulsion
Rectilinear fan
Conceptual design
Discretized Miller approach
Distortion tolerant fan

ABSTRACT

The performance benefits of directly ingesting the boundary layer (BLI) on air vehicles with distributed propulsion (DP) systems has been documented and explored extensively. However, numerous investigations have demonstrated that the increase of the flow distortion in the inlets of conventional propulsors can dramatically reduce the expected benefits. Hence, this work presents an alternative fan configuration to re-energize the boundary layer, and at the same time, to perform properly in a distorted and non-uniform flow-field. This conceptual design utilizes a two-dimension idealized fan and replaces the rotational movement with linear displacement, avoiding the undesired effects of circumferential distortion on the propulsor operation. A quasi two-dimensional model based on the Discretized Miller approach has been used to compare the proposed configuration with a conventional axial fan. From the results obtained, it is observed that the thermal performance of the fan is less affected for the proposed configuration and furthermore, intake pressure losses are ameliorated by the use of a single mailbox shape inlet. The performance assessment of the proposed configuration coupled on the N3-X aircraft shows benefits of 4% in fuel savings compared with current BLI turbomachinery configurations. The main contribution of this study lies on the definition of a preliminary design for an alternative propulsor configuration able to deal with circumferential distortion.

1. Introduction

The civil aviation sector has experienced a considerable growth in recent years since its important role in the market, business and tourism globalization. However, this also has resulted in a significant increase in air traffic, which in turn, has contributed to the increment of fuel consumption, gas emissions and noise pollution. The aforementioned issues, together with the fierce competitive pressures of the aviation industry, has driven engineers to develop and incorporate eco-friendly and more-efficient technological breakthroughs into multiple aeronautic design areas like aerodynamics [1] and propulsion [2]. In this context, the NASA N + 3 goals, which comprehend the third stage of an ambitious environmental project [3], has imposed on the aviation industry the reduction of the fuel burn in a specific time-frame.

To meet these environmental requirements, various futuristic upgrades for propulsion systems have been proposed. In particular, turbo electric distributed propulsion (TeDP) [4,5] and boundary layer ingestion (BLI) [6] are two concepts that have emerged as potential solutions to improve the propulsive efficiency and mitigate the aggressive fuel-burn of conventional aircraft. TeDP consists on replacing the net thrust that is provided by a large engine into small electrically-driven propulsors mounted on the trailing edge of the aircraft. These latter can be placed, sized and operated with greater flexibility than conventional fuel-powered engines[7], providing versatility for their integration into the airframe. On the other hand, the BLI technology enables the propulsors to ingest the boundary layer and re-energize the aircraft wake, resulting in the lessening of the overall power dissipation in the flow-field (kinetic energy wasted in the exhaust jet) [8]. The combined implementation of these breakthroughs has proven to be favorable in a sort of aspects like reduced wake drag, lower structural weight and less wetted area [1]. Numerous research has demonstrated that the installation of such technology results in a general diminution of 5–10% of burned fuel [9–11]. Shi et al. estimates a 4% decrease of the Thrust Specific Fuel Consumption (TSFC) when taking into account a TeDP system with BLI and considering nozzle, fan and inlets losses [12].

Nonetheless, the envisioned benefits of BLI configurations can be overshadowed if the flow-field distortion effects over the turbomachinery are not taken into account [10]. This issue is aggravated by

* Corresponding author.
E-mail address: esteban.valencia@epn.edu.ec (E. Valencia).

https://doi.org/10.1016/j.tsep.2020.100515

Nomenclature

A	Area, m^2
BC	Baseline configuration
BL	Boundary layer
BP_d	By pass ratio between ducts
BPR	Core-engine by pass ratio
BP	By pass ratio between free-stream and BL duct (indirect BLI case)
DP	Design point conditions
FPR	Fan pressure ratio
H_{CS}	Height of the capture sheet, m
K_{MT}	Mixing losses coefficient
l	length, m
M	Mach number
P	Total pressure, Pa
p	Static pressure, Pa
PW	Power,W
P	Total pressure, Pa
p	Static pressure, Pa
R	Gas constant, $\frac{J}{kg\,K}$
RB	Rotor Band configuration
TeDP	Turbo-electric distributed propulsion system
T	Total temperature, K
t	Static temperature, K
V	Velocity,m/s
w_{in}	Width of the intake, m
$()_d$	duct property
$()_1$	Inlet station
$()_t$	tip conditions
$()_r$	root conditions
$()_2$	Upstream fan station
$()_3$	Downstream fan station
$()_4$	Nozzle exit station,Inlet mixer station
$()_{4a} or ()_{4b}$	Inlet mixer station for free-stream and BL ducts respectively
$()_5$	Nozzle inlet station
$()_6$	Nozzle exit station
$()_{up}$	Parameter at uniform velocity profile condition
$()_{7^{th}}$	Parameter at 7^{th} law velocity profile condition
α	inlet air angle
β	exit air angle
γ	Heat capacity ratio
ε	deflection,$\alpha - \beta$

the associated intake pressure losses [13] due to the complex inlet configurations needed to re-arrange the incoming flow. Therefore, the design of fans able to work properly in highly-distorted flows (characteristic of the BLI) requires an extensive research focused on aerodynamics and material mechanics [14]. In this way, various authors have proposed different concepts to mitigate the dramatic drop of fan efficiency and mechanic performance. For instance, the Refs. [15–17,14,18,19] center their attention on the design of axial distortion tolerant fans by using stiffer and alternative blade designs. Conversely, other authors have proposed the design of non-axisymmetric stators with optimized outlet guide vanes [20,21]. However, the aforementioned studies share something in common; they have focused their research on aero-structural blade improvement using the conventional axial fan configuration.

On the contrary, this work tackles the distortion problem from a different perspective, changing the geometrical features of the propulsor by using a blade cascade architecture with linear displacement instead of the rotational axial configuration. This configuration transforms the three dimensional flow perceived by the fan blades into a two-dimensional flow. For this purpose, the blades are arranged in cascade and mounted over a band which displace linearly over the airframe trailing edge. Then, the exit flow is redirected to a row of fix blades (stator) located downstream the rotor band. The change of blade rotation for linear displacement reduces by one dimension the flow analysis and hence, circumferential distortion issues are avoided. For this reason, the velocity profile seen by the blades does not change for a determined flight condition and they can be shaped to optimize their performance. An scheme of the propulsor configuration is shown in Fig. 1.

It is important to mention that this work corresponds to a first insight of the proposed configuration and hence, parametric and quasi two-dimensional approaches with low computational costs, and high versatility for preliminary design stage have been used to assess its performance and suitability. In order to assess the performance characteristics of this alternative concept, the baseline aircraft (N3-X NASA concept) and the proposed rotor band configuration are modeled using the quasi two-dimensional Discretized Miller approach [13,22,23], which has been developed for conventional fans and, in this case, it is adapted for the linear fan configuration. Through these models, the fan's isentropic efficiency and power consumption are determined. As a figure of merit for the thermodynamic performance of the novel propulsion setup, the Thrust Specific Fuel Consumption (*TSFC*) parameter is computed using the TURBOMATCH Gas performance code developed by Cranfield University, which is coupled with the aforesaid propulsor performance modules.

2. Methodology

For the thermodynamic performance assessment of the proposed and baseline propulsion configurations, three main modules were developed: distortion assessment, propulsor performance and core-engine model. The first module works with the inlet flow conditions given by the baseline aircraft selected (NASA N3-X) and determines the fan geometry and performance characteristics, this module also allows to modify the percentage of BL re-energized (% BLI). The second module takes the fan features from the distortion module and assess the propulsor performance including the intake and nozzle losses, this module has thrust split (% TS), fan pressure ratio (FPR) and number of fans (n_{fan}) as main variables. The number of fans has been based on size-power limitations of expected electrical motors [24]. Finally, the core engine module uses as input the power required by the propulsors and has the engine by-pass-ratio (BPR) as main design space variable. Fig. 2 shows how these modules are coupled. It is important to highlight that the NASA N3-X aircraft [25] has been established as the baseline configuration, and since the aim of the present study is to highlight potential benefits of the rotor band configuration, three design space variables were set in the propulsion performance assessments: BPR is set to zero (turboshaft), %BLI equal to 100% (all the boundary layer flow is re-energized), %TS is one (all the thrust is delivered by the propulsor unit). In the next sections, each module is further described.

2.1. Baseline aircraft

In the present study, the conceptual Hybrid-Wing-Body aircraft NASA N3-X has been set as the baseline architecture. This aircraft incorporates futuristic technology in what respect to propulsion configurations, composite materials, electric motors technology, and thermal management systems. For instance, the baseline aircraft is expected to integrate turbo-electric distributed propulsion (TeDP), boundary layer ingestion (BLI), ceramic-matrix-composites (CMC), High-Temperature-Superconductive (HTS) electric motors, and liquid hydrogen cryo-cooling systems [25–27]. It is envisaged the advancement of the

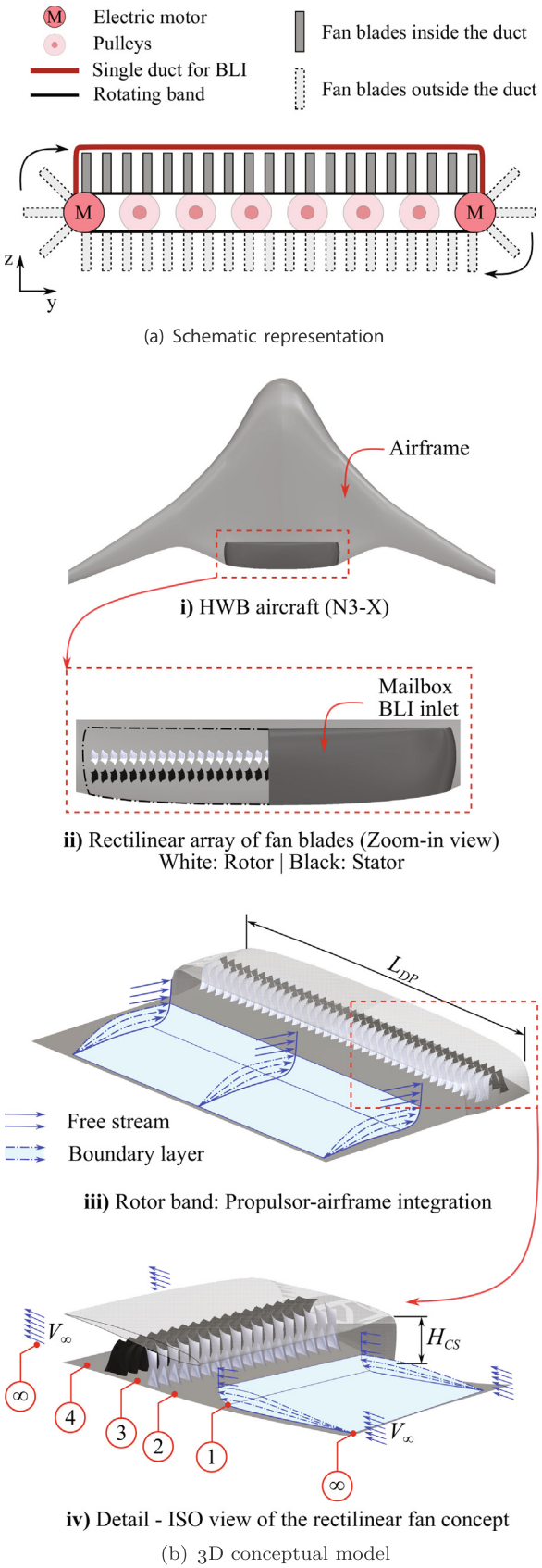

Fig. 1. Rotor band: propulsion – airframe integration.

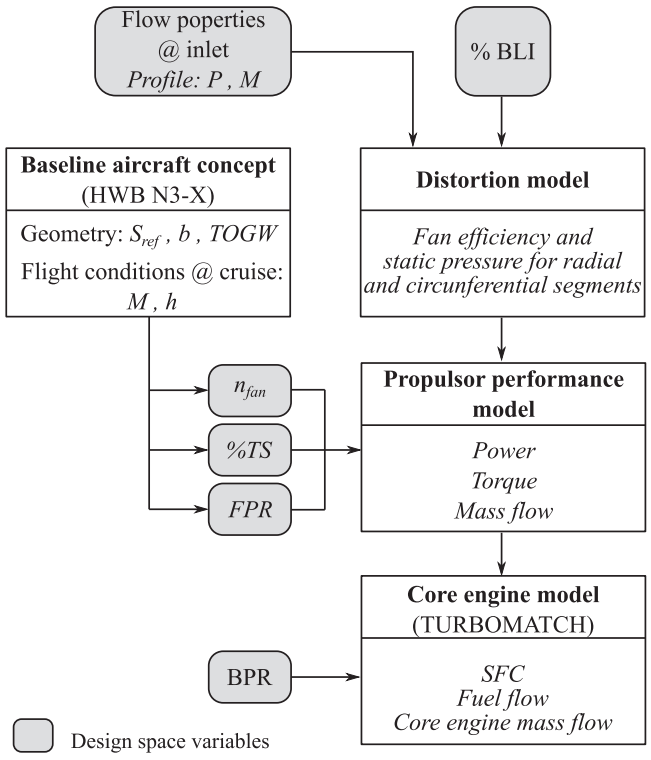

Fig. 2. Performance analysis methodology.

aforesaid technologies will permit the NASA N3-X aircraft to meet the N + 3 goals, regarding the reduction of fuel consumption and emissions [28,29]. As this work focuses on the propulsor performance analysis, the flight conditions, airframe configuration and HTS system of the NASA N3-X aircraft have been maintained and are described in Table 1. The work undertaken here employs a previously developed method that uncouples the airframe and the propulsion system [30]. This approach permits computing relevant parameters of a TeDP aircraft with BLI system by uncoupling the airframe and the propulsion system in independent modules. Nevertheless, both modules are linked by the flow properties entering into the propulsion module control volume, which have been taken from the CFD analysis of the N3-X airframe [25]. Specifically the data used to characterize the flow are the incoming Mach number and total pressure profiles. These flow features allow to characterize the fan's performance through the Discretized Miller approach [13], which discretizes in streams the flow and enables the assessment of the circumferential and radial distortion produced by the distorted inlet flow. The quasi two dimensional nature of the Discretized Miller approach reduces computational cost and can be easily embedded into the fan performance module. The thermodynamic performance of the baseline and proposed configurations is assessed using the TURBOMATCH gas performance code based on the studies carried out in Ref.[22], which defined the performance benefits of conventional distributed propulsor configurations (axial fans) with BLI for the N3-X aircraft concept. Reference [22] also highlighted the effect of different thrust split configurations and how they affect the benefits accrued from BLI. For this study, the baseline and proposed configurations are modeled with 98% thrust split (the required thrust is delivered by the distributed propulsors). In addition the TURBOMATCH code models a 3-spool turboshaft with free power turbine. For the sake of convergence in the gas turbine performance code, each turboshaft was modelled as each one delivers a small amount of thrust (approximately 1% of the intrinsic net thrust). Since the baseline configuration requires a number of fans (propulsors) as input, their number was defined based on the geometrical space limitations for their allocation at the airframe trailing edge, they vary ranging from 15–20 in fuction of the pressure ratio. For

Table 1
Performance and operational characteristics of the baseline aircraft NASA N3-X and its propulsion system.

	Parameter	Value		Parameter	Value
General	Number of passengers	300	Power Plant	Two turbo-shaft engines	
	Maximum payload	118 [t]	HTS system	Cryo-cooling system with liquid H_2	
Performance[a]	Range	13890 [km]	Propulsors	Thrust split	98%
	Flight altitude	12192 [m]		FPR	1.15–1.45
	Flight speed	0.84 Mach		Number of fans	15–21
	Intrinsic net thrust	73.9 [kN]			

[a] Corresponding to cruise conditions.

the fan hub radius calculation two synchronous electric model motors [31,32,24] were used.

2.2. Rotor band assessment

A similar approach, as those presented in Refs. [30,22], is employed for assessing the performance of the rotor band concept. In order to allow a fair comparison of the propulsion systems the NASA N3-X aircraft concept is considered for the rotor band assessment. Hence the incoming flow properties and propulsion unit location are assumed the same. However, a main difference is that the rotor band case has a lower number of rectilinear fans (in this case only one), therefore instead of using number of fans as variable, the length of the propulsor was considered as design variable. The integration of the proposed architecture into the propulsor system is illustrated in Fig. 1b, where both the rotor and stator blades can be appreciated. Regarding the core engine module the same considerations as the baseline configuration are taken.

It is important to note that, at this early stage of design, the purpose is to highlight the potential benefits of reducing both distortion and pressure losses in BLI configurations. Thus, this work focuses on the rotor band conceptual design rather than a deep analysis of the specific arrangements for the concept presented, the only variable accounted in this work for its geometrical definition is its length, which is mainly due to its direct effect over intake losses and fan performance, since it affects the BL capture sheet height.

2.2.1. Propulsor performance model

This model calculates the propulsor performance using the method defined in Ref. [13]. Analogously to the aforementioned reference, an internal control volume that encloses the propulsor unit [33,30] is used and the inlet flow properties are defined based on the baseline aircraft calculations. This module works together with the Distortion module, which defines the fan geometry and blade performance following of the Discretized Miller approach defined in Ref. [13] adapted for the case of a linear blade cascade. The next section describes this method and also, enlists some assumptions for the aerodynamic integration.

Aerodynamic integration To evaluate the propulsor performance, the inlet flow properties are assumed to be equal to the BL characteristics (Table 1), which in turn were calculated based on the velocity profiles provided by Felder et al. [25]. Moreover, to simplify the analysis, the ingested flow properties at station 1 (Fig. 1(b) – bottom) are assumed that has not been either diffused or compressed within the stream-tube entering the intake [26]. In other words, the height of the intake is equal to the height of the capture sheet before any diffusion or compression has taken place (Fig. 1(b) – bottom). The Mach number and the inlet total pressure are calculated using Eqs. (2) and (1) respectively [25] and the intake pressure drop is calculated based on Eq. (3). For the blade design, the mass averaged values of these properties are utilized. Then, in order to define the height of the boundary layer ingested, the capture sheet height (H_{CS}) is utilized as handle in an iterative calculation. As the length of the propulsor (L_{DP}) is defined, the capture sheet height can be calculated using the continuity equation. Figs. 3 and 1 show the methodology and intake configuration respectively.

$$M_{BL} = M_1 = M_\infty \left(\frac{y}{\delta}\right)^{1/11} - 0.14 \tag{1}$$

$$P_{BL} = P_1 = P_\infty \left(\frac{y}{\delta}\right)^{1/15} - 0.075 \tag{2}$$

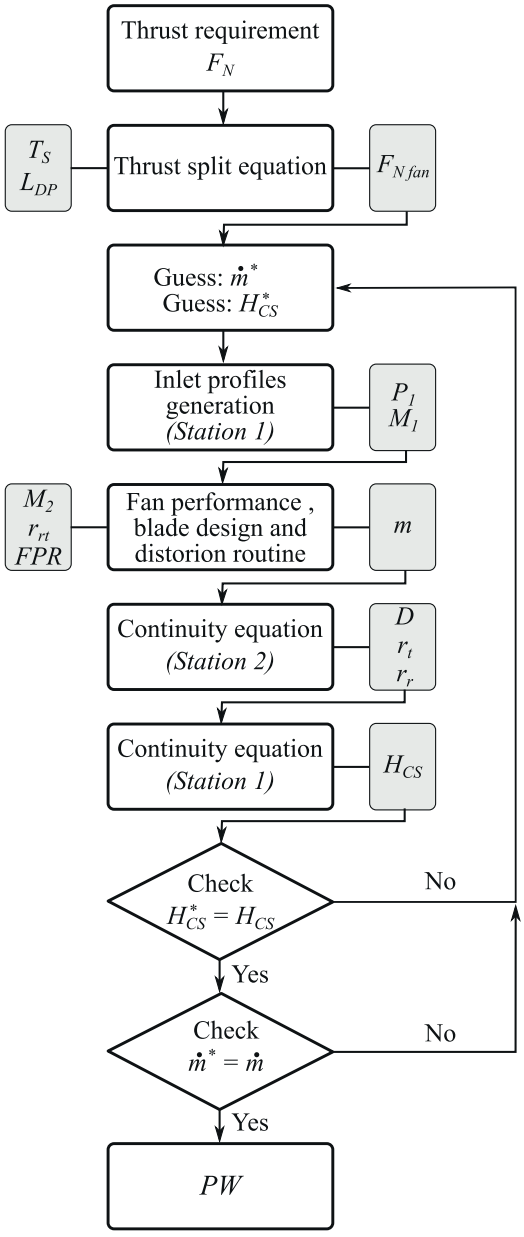

Fig. 3. Propulsor performance methodology.

$$\Delta P_{in} = \frac{\Delta P_{1-2}}{P_1} \tag{3}$$

In order to calculate the intake pressure losses for the propulsor performance module a subroutine based on a parametric approach is developed for the axial and rectilinear fan cases. This was implemented since, as observed in previous studies [30], the intake pressure losses play an important role in the calculation of BLI benefits.

Intake pressure losses The effect of intake pressure losses over the system performance has been examined in previous works [13,30] and it has been found that they affect in large extent the overall propulsor performance. For this reason, they are considered in the comparison between the alternative and baseline concepts. Although the detailed intake configuration in both cases is unknown, the geometrical variations produced by the change of the fan configuration allow to calculate and compare the intake wetted areas in both cases. These wetted areas can be used to define the intake pressure recovery for each case. This process is not accurate enough to give the actual pressure losses, but it is useful to give an insight of the pressure loss magnitude for each configuration and capture main trends that will enable to note the benefits of using these two propulsor configurations at preliminary design stage. The following equations are utilized in the present work to analyze the pressure losses and they are derived based on definitions found in the public domain [34]. Fig. 4 shows the parameters utilized in these equations.

$$\Delta P_{in} = \frac{1.328}{Re_c^{0.5}} f I \tag{4}$$

where f is given by Eq. 5

$$f = \frac{4(\alpha_d 180/\pi)^2}{125} - \frac{3(\alpha_d 180/\pi)}{100} + 1 \tag{5}$$

Re_c and I for the rotor band are given by

$$Re_c = \frac{2V_1 l_d \rho_1}{\mu} \tag{6}$$

$$I = \frac{(h - l_d tan(\alpha_d))^2}{cos(\alpha_d)} \int_0^l \frac{dx}{(h - l_d tan(\alpha_d) + x tan(\alpha_d))^3} \tag{7}$$

and for the axial fan configuration they are given by

$$Re_c = \frac{2V_1 (r_t - l_d tan(\alpha_d))\rho_1}{\mu} \tag{8}$$

$$I = \frac{2(r_t - l_d tan(\alpha_d))^4}{cos(\alpha_d)} \int_0^l \frac{dx}{(r_t - l_d tan(\alpha_d) + x tan(\alpha_d))^5} \tag{9}$$

The distortion module generates a matrix of values for fan efficiency and static pressure increment in vertical and transverse directions. These values are mass averaged and the fan downstream properties are calculated. The mass flow through the propulsor can be calculated with the intrinsic net thrust of the propulsor, which has been assumed for this study at cruise condition. By doing this, the power consumed by the propulsor unit can be defined and this later on, is feed to the core-engine module, which will be in charge of delivering the required power to the propulsor unit for the set operating condition.

2.2.2. Distortion model

The effects of the distorted inlet flow over the fan performance are assessed through the Discretized Miller approach [13], which evaluates the flow performance for radial and circumferential discretized streamlines. For the rotor band, blades move linearly and the discretization process only is needed in the blade spanwise direction, as the blade passages present similar behaviour. For the rectilinear fan blade design a parametric meanline analysis using semi-empirical correlations [35,36,13] is used and since the blade passsages perceive the same incoming flow characteristics they can be shapped accordingly to optimize their performance at determined flight condition (this does not happen in conventional axial fans due to circumferential distortion imposed by BLI). This simplifies and reduce computational cost because only one blade passage needs to be calculated. For the case of conventional axial fans off-design (*OD*) refinement correlations are needed to assess the performance of the blade passages operating under distorted conditions, as can be observed in Fig. 5. Fig. 5 a shows a schematic discretization of the blade passages and the 3D velocity profiles and as observed for the case of the conventional fan *OD* conditions are present at all the spanwise locations with exception of the meanline region (DP design), whilst for the rectilinear fan all the spanwise sections can be computed with DP correlations (Fig. 5b).

Blade design and fan performance For the conventional axial fan design as previously explained it is needed off design considerations, which were determined using Carter's rule [37], where the deviation angle is calculated as a function of the stagger and camber angles through empirical charts based on the methodology described by Howell [38] and Miller [23].

With the blade geometry for rectilinear and conventional fans determined, the minimum loss (ml), optimum stall and choke incidence angles are calculated. The loss coefficient calculation in the method follows the approach as described in the work of Howell [38], Miller [23] and White [39], which used the loss calculations of the following correlations. For the total loss coefficient for minimum loss (ω_{ml}), the deviation angle for off-design conditions (δ_{OD}), the total loss coefficient for off-design conditions (ω_{OD}) were based on Miller [23] approach. Meanwhile, for end wall loss coefficient (ω_{ew}) and for profile loss coefficient (ω_p) were based on the Wright method [40]. Finally, for the shock wave loss coefficient (ω_{sw}) the Schwenk's technique [41] was employed. The loss coefficient definition used in the fan performance calculation is given by Eq. (10) and is based on studies conducted by Howell [38], Miller [23] and Osborn [42]. The total loss coefficient is given as follows:

$$\omega = \frac{\Delta P_{ideal} - \Delta P_{real}}{P'_{LE} - P_{LE}} = \omega_p - \omega_{sec} \tag{10}$$

where ω_p and ω_{sec} stands for profile and secondary losses, respectively. The secondary losses implemented in the model correspond to the end wall and shock wave effects. The ideal static pressure increment is calculated based on the assumption of constant relative total pressure across the rotor or constant total pressure for the case of the stator.

For the Discretized Miller analysis undertaken for the rectilinear fan the definitions of losses previously explained are adapted for the case of only one dimension variation in flow properties (spanwise direction). The loss coefficient definitions for profile and end wall losses in the discretized of the rectilinear fan model are:

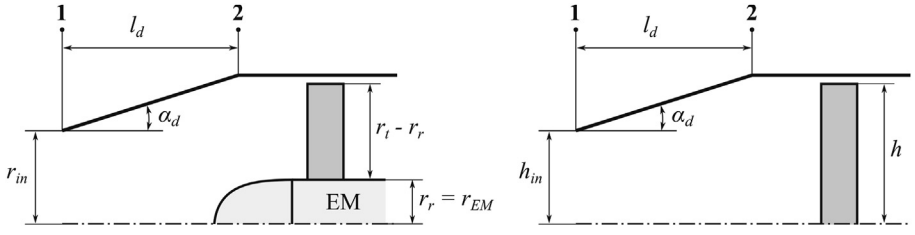

Fig. 4. Intake configuration for baseline (left) and rotor band (right) cases.

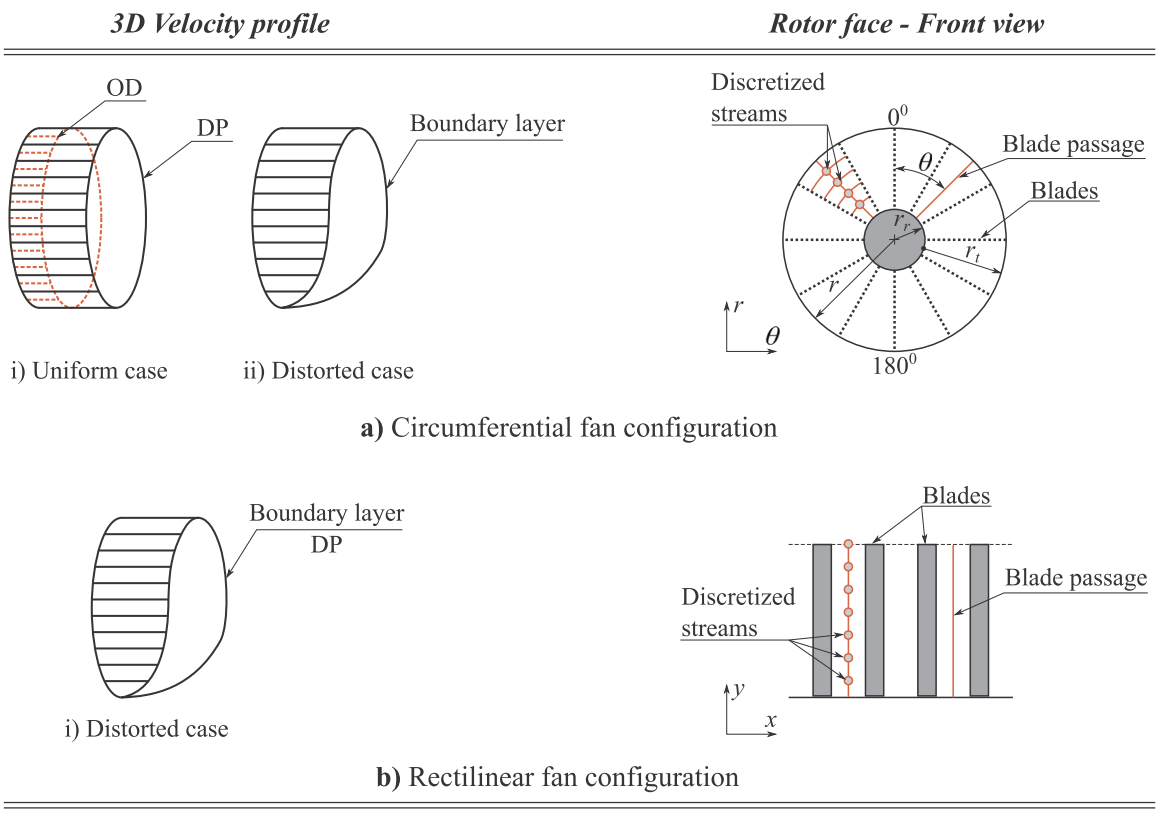

Fig. 5. Discretization of the streams in the blade passage for axial and rectilinear configurations.

$$\omega_p(h) = \frac{\omega_{p,par}(h)}{0.5\left(\frac{V_{LE}(h)}{V_{TE}(h)}\right)^2 cos(\beta_{TE}(h))} \tag{11}$$

$$\omega_{ew}(h) = \frac{\omega_{ew,par}(h)}{0.5\left(\frac{V_{LE}(h)}{V_{TE}(h)}\right)^2 \frac{h}{c}} \tag{12}$$

where $\omega_{p,par}$ (for end wall and profile losses) corresponds to the total loss parameter and depends on the diffusion factor [40]. Similar to equations for calculating loss coefficients, the diffusion factors are also calculated as a function of the position in the flow. In Eqs. (11) and (12), the term h is defined by the number of stations along the blade span (Fig. 5).

It is worth to mention that this work considers fan pressure ratios between 1.15 and 1.5, a span-wise constant whirl velocity design and the geometrical features in Table 2.

As the fan assembly for this study presents one stage and is expected to operate at low pressure ratio, the density variation and blockage effects across the blade arrangement are neglected [36]. These assumptions essentially simplify the model by enabling the use of incompressible flow equations. These relations in turn can be used to calculate the static pressure increment.

The calculation of this latter is given by Eq. (13), which is function of the relative flow velocities at the exit of rotor and stator [1]. This static pressure increment in the blade frame of reference is equal to the total pressure increment in the absolute frame as the axial velocity is assumed constant through the fan (no dynamic pressure increment).

$$\Delta p_{th} = \frac{\Delta p_{2-3}}{1/2\rho V_2^2} = \left(1 - \frac{V_3^2}{V_2^2}\right) \tag{13}$$

The real static pressure increment is calculated by subtracting the aforementioned losses to the theoretical pressure increment. For the case of the rectilinear fan, the annular and secondary losses are expected to change as it does not rotate. For this reason, their contribution is assessed in the results section. Finally with the real and ideal static pressure increments, the fan efficiency can be computed.

Table 2
Blade design parameters.

Parameter	Value
Aspect ratio(AR)	2.86
Root to tip ratio (r_H)	0.4
Incidence rotor (i_r) [^{0}]	0
Incidence stator (i_s) [^{0}]	0

Similarly to reference [22], the parametric nature of the model and semi-empirical correlations for losses constrain up to certain extent the accuracy improvements and hence, it is used the same number of streams as the previous study, where 10 streams are used.

Then with the fan performance parameters (FPR and η_f) determined the performance module takes these values and carries out the propulsor performance analysis as depicted in Fig. 3.

2.3. Core-engine model

The engine model utilized in this analysis is a turbo-shaft engine of 3-spools with a free power turbine as shown in Fig. 6. The engine model assume a futuristic level of technology [25,26] and some of its parameters are described in Table 3.

The aim of this study is to assess the benefits of the alternative fan configuration and hence, the effect of the core-engine variables is not assessed in the present work. In order to avoid convergence issues in the core-generator model, the thrust split for all the cases is set at 98%.

[1] The velocities presented in this equation are relative to the blade

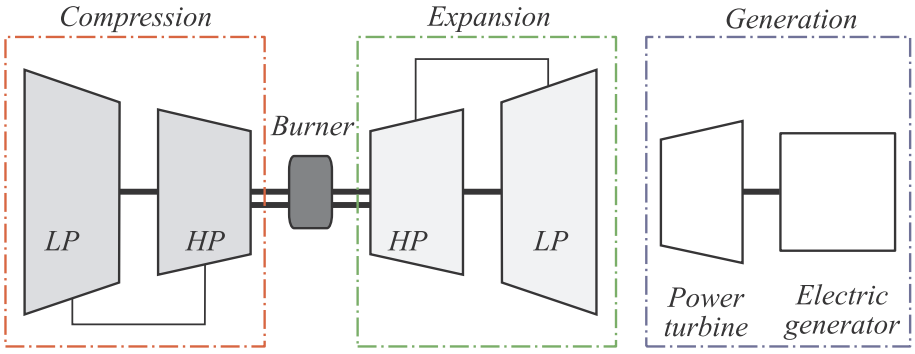

Fig. 6. Core-engine configurations.

Table 3
Core-engine specifications at DP [25].

Parameter	Value
Overall pressure ratio (OPR)	75
Turbine inlet temperature (TET) [K]	1727.7
Burner efficiency (η_{comb})	0.998
LP compressor polytropic efficiency	0.932
HP compressor polytropic efficiency	0.932
LP turbine polytropic efficiency	0.93
HP turbine polytropic efficiency	0.93
Power turbine polytropic efficiency	0.924

3. Results and discussions

In this section the results and discussion for the fan performance model and the system performance are presented. In this latter the core-generator model is utilized in order to define the *TSFC*.

3.1. Propulsor performance analysis

In this section the results regarding the performance of the distributed propulsors are shown.

Intake pressure losses analysis Fig. 7 shows the pressure losses for the rectilinear fan or rotor band (RB) and the baseline configuration (BC). The duct length(l_d) and duct inclination angle (α_d) are also incorporated as variables in order to assess the increment in pressure losses due to the intake geometry.

As can observed in Fig. 7 the baseline case which uses axial fans with separate ducts presents larger pressure losses than the single intake duct of the rotor band configuration. This can be attributed to the large wetted areas of individual propulsors. Although this pressure loss calculation is based on a basic the intake geometry, it shows that the rotor band intakes present a higher recovery pressure than the axial fan configurations. This should be refined with the actual intake geometries, so the results obtained can be closer to the real performance. However, this study is beyond the scope of the present work where only a preliminary design was carried out.

Distortion effect over fan performance The displacement movement that the rotor band presents will influence the secondary and annular losses. Fig. 8 shows the effect of the losses produced by these components on the fan efficiency at different fan pressure ratios. The comparison of the fan efficiency for the baseline and rotor band case is shown in Fig. 9.

The effect of neglecting the annular and secondary losses can be observed in Fig. 8. In this case, the improvement in fan efficiency contributes to enlarge the benefits that this new configuration could bring compared with conventional distributed propulsion architectures. Hence, at preliminary design stage, this configuration highlights a potential enhancement, which will need to be verified using higher fidelity methods like either experimental or CFD.

In the rotor band configuration, the fan blades are designed to deliver the same whirl velocity component to the flow at different blade spans. As the rotor band blades present the same tangential velocity along their span, the flow coefficient (C_a/U) of the blade tip reduces in comparison with the axial fan case. This lower flow coefficient increase the inlet blade angle and the deflection at this blade span location, hence reducing the pressure losses. In other words, the two dimensional blade design assumed in this work performs better with the low axial velocity section of the velocity profile (boundary layer) than with the high axial velocity region (free-stream). For this reason, the cases of lower capture sheet height (longer propulsor and less free-stream ingested), presents a slightly better mass averaged fan efficiency an hence, better propulsor performance, as shown in Figs. 9 and 10 respectively. Furthermore, the variation of the capture sheet height for the two propulsor lengths shows that reducing the capture sheet height by 55% requires an increment in propulsor length of 55% at the lowest FPR analyzed. This is something to take into account in the design of this propulsion concept, since in order to perform better than the axial fan case, it requires a capture sheet height smaller than the one of axial fans. This means that the rotor band will occupy a larger space in the airframe. The small capture sheet height is required for the rotor band concept in order to reduce the region of low flow coefficient going through the fan, as this issue affects the fan performance as was explained in the previous paragraph.

Propulsor performance Fig. 10 shows the effect of the secondary

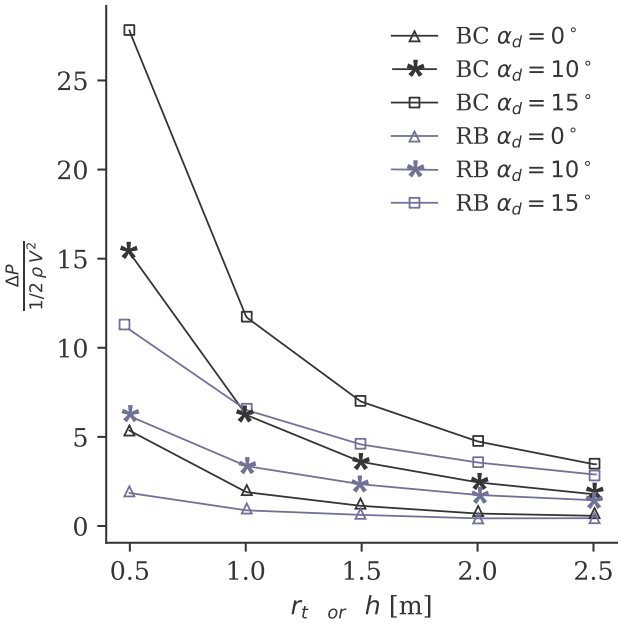

Fig. 7. Predicted pressure losses based on the intake wetted area for the baseline and rotor band configurations.

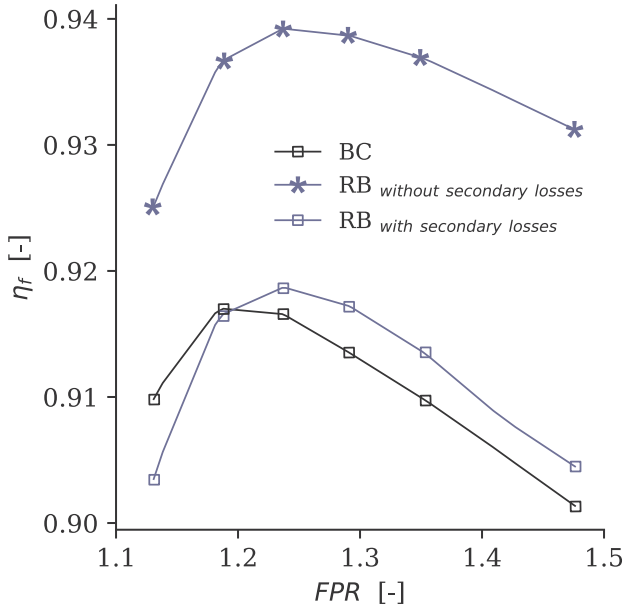

Fig. 8. Effects of secondary and annular losses over fan efficiency at different fan pressure ratios.

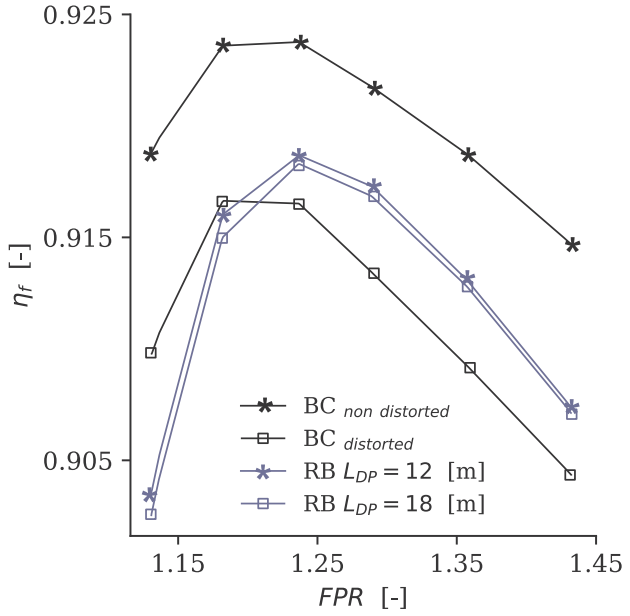

Fig. 9. Fan efficiency for baseline and rotor band cases at different fan pressure ratios.

and annular losses in the power consumed by the distributed propulsors. The capture sheet height for two rotor band configurations and the baseline configuration is shown in Fig. 11.

3.2. Propulsion system performance

The effect in *TSFC* of the propulsor length in the rotor band configuration and its comparison with the baseline configuration are shown in Figs. 12 and 13 respectively. Fig. 13 shows the *TSFC* for the rotor band cases when secondary and annular losses are taken into account.

As mentioned previously in the rotor band configuration, the constant tangential blade velocity along the span produces large losses at the locations working with higher axial velocity (tip), which decreases the mass averaged fan efficiency. The effect of reducing these losses and

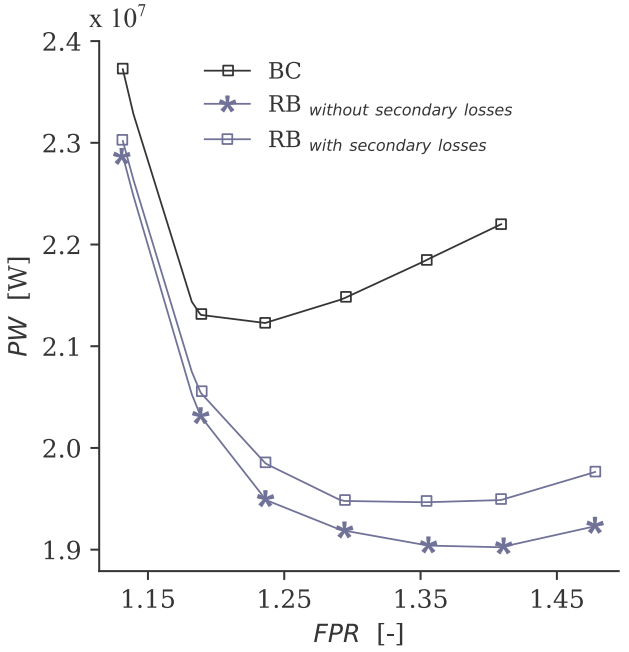

Fig. 10. Effects of secondary and annular losses over power required by the fan at different fan pressure ratios.

momentum drag over the fan performance is observed in Figs. 12 and 13. This latter Figure highlights the combined benefit of the aforementioned issues and hence, a reduction in *TSFC* of approximately 5%, which represents enormous benefits when extrapolated at civil aircraft levels. Therefore, it can be summarized that the concept developed presents potential opportunities, which need to be further explored in order to assess definitely its suitability for the propulsion of advanced concepts as the N3-X. As mentioned before, this work was focused on the design and preliminary performance assessment of this novel configuration and hence, it is required to develop refined assessments with higher fidelity tools to corroborate the benefits predicted.

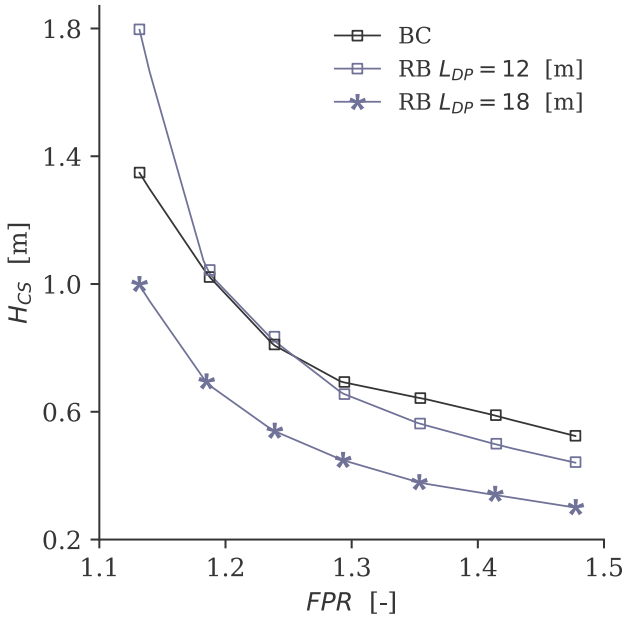

Fig. 11. Capture sheet height for baseline and rotor band configurations at different fan pressure ratios.

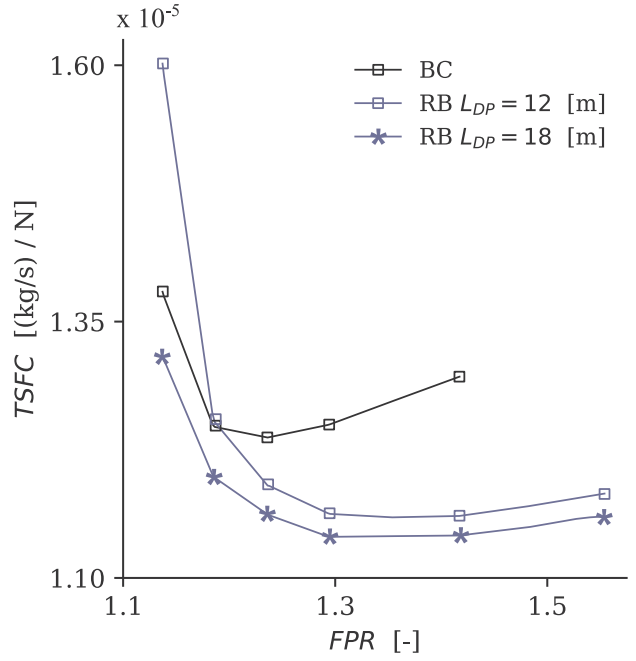

Fig. 12. *TSFC* for rotor band for different propulsor lengths and for the baseline case.

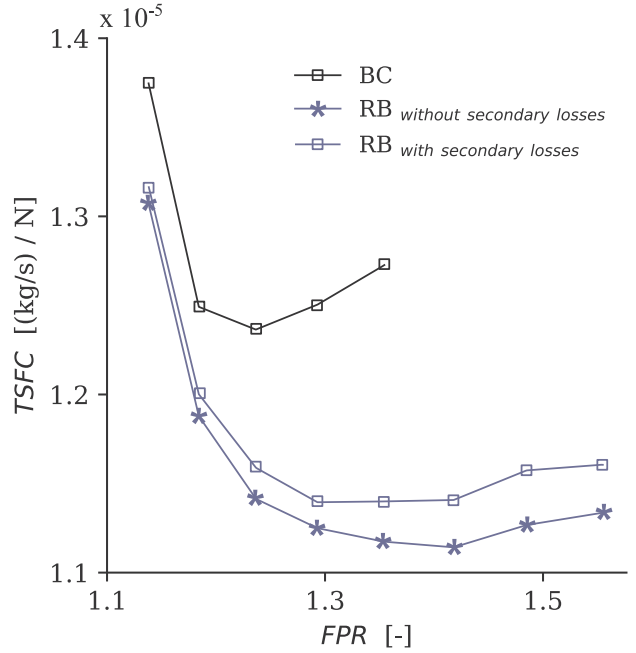

Fig. 13. *TSFC* for rotor band for different loss components and for the baseline case.

3.3. Electrical system

The electrical equipment envisioned for this future aircraft concept has been examined previously and their characteristics have been defined to certain extent in Refs. [43,28,24]. Similar to the baseline aircraft, HTS electric motors, thermally managed by liquid hydrogen cryocoolers, have been considered for the rectilinear fan configuration to drive the rectilinear array of blades. In the case of distributed propulsion with conventional axial fans, it has been determined that some configurations are only possible with highly optimistic assumptions regarding power-train, electric motor and cooling technology [13,44,45]. In the case of the rotor band configuration, the linear movement represent an advantage, since there is not a link between rotational speed and blade radius. This means that the blade height is independent of the electrical motor rotational speed. This independence on blade root-to-tip ratio enables any geometrical combination between blade geometry and electrical motors characteristics. For this reason, in the rotor band case, the propulsor length can be shifted without compromising the feasibility of the propulsion unit architecture.

4. Conclusions

An alternative fan configuration for a distributed propulsion system with BLI has been developed and its performance has been assessed using the streamline method, which is based on semi-empirical relations and fan design. The preliminary results indicate that a reduction in 5% in *TSFC* can be achieved depending on the length of the propulsor utilized. This benefit is attributed to the reduction in capture sheet height and hence momentum drag that a longer propulsor requires.

The alternative fan configuration presents a similar fan efficiency drop than the conventional axial fans due to BLI. This is caused by the low flow coefficient at the blade tip that generates large pressure losses reducing the mass averaged fan efficiency. However further refinement in the two dimensional blade design is necessary to assess the change in annular and secondary losses for non rotational blades, as they could improve or affect in large extent the fan performance.

The case of a large propulsor intake in the rotor band configuration is expected to present lower pressure losses than the case of separated intakes in the axial fan configuration, due to the reduction in wetted area. The expected lower intake pressure losses for the alternative configuration is an important aspect, as it improves the performance of BLI distributed propulsion systems in large extent.

The results obtained show that the rotor band configuration is a promising concept, which needs to be further studied in order to determine in more detail its suitability for future aircraft concepts with BLI and TeDP. Furthermore, it is important to note, that this work is a first step where on a conceptual novel design for a distortion tolerant fan is explored, hence only main performance parameters were calculated to assess its suitability, however alternative configurations for this setup can be studied in further stages to integrate better the benefits at aircraft performance levels, some possibilities are: reciprocant BLI rectilinear fan with only one row of blades, BLI in both airframe surfaces, among others; these different setups need to be explored further as they can bring new opportunities.

CRediT authorship contribution statement

Esteban Valencia: Conceptualization, Funding acquisition, Methodology, Writing - original draft. **Victor Alulema:** Data curation. **Dario Rodriguez:** Data curation. **Panagiotis Laskaridis:** Writing - review & editing. **Ioannis Roumeliotis:** Software.

Declaration of Competing Interest

The authors declare that they have no known competing financial interests or personal relationships that could have appeared to influence the work reported in this paper.

Acknowledgements

The authors gratefully acknowledge the financial support provided by Escuela Politécnica Nacional for the development of the internal projects: PIMI 15-03 and PIMI 18-01. Furthermore, the authors thank the Cranfield Departamental grant for financial support and Prof. Emeritus Riti Singh for sharing his broad experience and insights for the development of the present work.

References

[1] A. Abbas, J. De Vicente, E. Valero, Aerodynamic technologies to improve aircraft performance, Aerosp. Sci. Technol. 28 (1) (2013) 100–132.
[2] A.K. Sehra, W. Whitlow, Propulsion and power for 21st century aviation, Prog. Aerosp. Sci. 40 (4–5) (2004) 199–235.
[3] S.W. Ashcraft, A.S. Padron, K.A. Pascioni, G.W. Stout Jr., D.L. Huff, Review of propulsion technologies for N+ 3 subsonic vehicle concepts (Tech. rep.), NASA Glenn Research Center, 2011.
[4] A.T. Wick, J.R. Hooker, C.H. Zeune, Integrated aerodynamic benefits of distributed propulsion, 53rd AIAA Aerospace Sciences Meeting, 2015, p. 1500.
[5] P. Laskaridis, Assessment of distributed propulsion systems used with different aircraft configurations, 51st AIAA/SAE/ASEE Joint Propulsion Conference, 2015.
[6] K.M. Sabo, M. Drela, Benefits of boundary layer ingestion propulsion, In 53rd AIAA Aerospace Sciences Meeting, 2015.
[7] H.D. Kim, A.T. Perry, P.J. Ansell, A review of distributed electric propulsion concepts for air vehicle technology, 2018 AIAA/IEEE Electric Aircraft Technologies Symposium, 2018.
[8] A. Uranga, M. Drela, E.M. Greitzer, D.K. Hall, N.A. Titchener, M.K. Lieu, N.M. Siu, C. Casses, A.C. Huang, G.M. Gatlin, J.A. Hannon, Boundary layer ingestion benefit of the D8 transport aircraft, AIAA J. 55 (11) (2017) 3693–3708.
[9] G. Brown, Weights and efficiencies of electric components of a turboelectric aircraft propulsion system, 49th AIAA Aerospace Sciences Meeting including the New Horizons Forum and Aerospace Exposition, AIAA, 2011.
[10] A. Plas, M. Sargeant, V. Madani, D. Crichton, E. Greitzer, T. Hynes, C. Hall, Performance of a Boundary Layer Ingesting (BLI) propulsion system, 45th AIAA Aerospace Sciences Meeting and Exhibit, AIAA, 2007.
[11] R.T. Kawai, D.M. Friedman, L. Serrano, Blended Wing Body (BWB) Boundary Layer Ingestion (BLI) inlet configuration and system studies (Tech. rep.), NASA Langley Research Center, 2006.
[12] M. Shi, M. Pokhrel, J. Gladin, E. Garcia, D.N. Mavris, Model fidelity requirements in boundary layer ingestion propulsion system conceptual design, 2018 Aviation Technology, Integration, and Operations Conference, 2018.
[13] E. Valencia, V. Hidalgo, D. Nalianda, P. Laskaridis, R. Singh, Discretized Miller approach to assess effects on boundary layer ingestion induced distortion, Chin. J. Aeronaut. 30 (1) (2017) 235–248.
[14] M. Bakhle, T. Reddy, G. Herrick, A. Shabbir, R. Florea, Aeromechanics analysis of a boundary layer ingesting fan, 48th AIAA/ASME/SAE/ASEE Joint Propulsion Conference & Exhibit, 2012.
[15] W.T. Cousins, D. Voytovych, G. Tillman, E. Gray, Design of a distortion-tolerant fan for a boundary-layer ingesting embedded engine application, 53rd AIAA/SAE/ASEE Joint Propulsion Conference, 2017.
[16] R.V. Florea, D. Voytovych, G. Tillman, M. Stucky, A. Shabbir, O. Sharma, D.J. Arend, Aerodynamic analysis of a boundary-layer-ingesting distortion-tolerant fan, ASME Turbo Expo 2013: Turbine Technical Conference and Exposition, American Society of Mechanical Engineers Digital Collection, 2013.
[17] D. Perovic, Distortion Tolerant Fan Design (Ph.D. thesis), University of Cambridge, 2019.
[18] M. Pokhrel, M. Shi, J. Ahuja, J. Gladin, D.N. Mavris, Conceptual design of a bli propulsor capturing aero-propulsive coupling and distortion impacts, AIAA SciTech 2019 Forum, 2019, p. 1588.
[19] M. Mennicken, D. Schönweitz, M. Schnoes, R. Schnell, Conceptual fan design for boundary layer ingestion, ASME Turbo Expo 2019: Turbomachinery Technical Conference and Exposition, American Society of Mechanical Engineers Digital Collection, 2019.
[20] E.J. Gunn, C.A. Hall, Nonaxisymmetric stator design for boundary layer ingesting fans, J. Turbomach. 141 (7) (2019) 1–10.
[21] S. Kumar, M.G. Turner, K. Siddappaji, M. Celestina, Aerodynamic design system for non-axisymmetric boundary layer ingestion fans, Proceedings of the ASME Turbo Expo, 2018, pp. 1–7.
[22] E.A. Valencia, C. Liu, N. Devaiah, P. Laskaridis, I. Gray, R. Singh, Methodology for the assessment of distributed propulsion configurations with boundary layer ingestion using the discretized miller approach, Int. Rev. Aerospace Eng. 10 (3) (2017) 174–187.
[23] D. Miller, D. Wasdell, Off-design prediction of compressor blade losses, IMECHE (1987) p. C279/87.
[24] C.A. Luongo, P.J. Masson, T. Nam, D. Mavris, H.D. Kim, G.V. Brown, M. Waters, D. Hall, Next generation more-electric aircraft: a potential application for hts superconductors, IEEE Trans. Appl. Supercond. 19 (3) (2009) 1055–1068.
[25] J. Felder, H. Kim, G. Brown, J. Kummer, An examination of the effect of boundary layer ingestion on turboelectric distributed propulsion systems, 49th AIAA Aerospace Sciences Meeting including the New Horizons Forum and Aerospace Exposition, 2011, pp. 1–26.
[26] H. Kim, J. Felder, Control volume analysis of boundary layer ingesting propulsion systems with or without shock wave ahead of the inlet, 49th AIAA Aerospace Sciences Meeting Including the New Horizons Forum and Aerospace Exposition, 2011, p. 222.
[27] J. Felder, M. Tong, J. Chu, Sensitivity of mission energy consumption to turboelectric distributed propulsion design assumptions on the n3–x hybrid wing body aircraft, 48th AIAA/ASME/SAE/ASEE Joint Propulsion Conference & Exhibit, 2012.
[28] M.J. Armstrong, C.A. Ross, M.J. Blackwelder, K. Rajashekara, Propulsion System Component Considerations for NASA N3-X Turboelectric Distributed Propulsion System, SAE Int. J. Aerospace 5 (2) (2012) 344–353.
[29] J. Felder, H. Kim, G. Brown, Turboelectric distributed propulsion engine cycle analysis for hybrid-wing-body aircraft, 47th AIAA Aerospace Sciences Meeting including The New Horizons Forum and Aerospace Exposition, 2009, pp. 1–25.
[30] E.A. Valencia, D. Nalianda, P. Laskaridis, R. Singh, Methodology to assess the performance of an aircraft concept with distributed propulsion and boundary layer ingestion using a parametric approach, Proc. Inst. Mech. Eng. Part G 229 (4) (2015) 682–693.
[31] P.J. Masson, D.S. Soban, E. Upton, J.E. Pienkos, C.A. Luongo, HTS motors in aircraft propulsion: design considerations, IEEE Trans. Appl. Supercond. 15 (2 PART II) (2005) 2218–2221.
[32] C.A. Snyder, J.J. Berton, G.V. Brown, J.L. Dolce, M.V. Dravid, D.J. Eichenberg, J.E. Freeh, C.A. Gallo, S.M. Jones, K.P. Kundu, et al., Propulsion Investigation for Zero and Near-Zero Emissions Aircraft (Tech. rep.), NASA Langley Research Center, 2009.
[33] D. Rodriguez, A multidisciplinary optimization method for designing boundary layer ingesting inlets, Symposium on Multidisciplinary Analysis and Optimization, AIAA/ISSMO, 2002.
[34] E.L. Goldsmith, J. Seddon, Practical Intake Aerodynamic Design, Blackwell Scientific, Oxford, 1993.
[35] S.L. Dixon, C. Hall, Fluid Mechanics and Thermodynamics of Turbomachinery, Butterworth-Heinemann, 2013.
[36] H.I.H. Saravanamuttoo, G.F.C. Rogers, H. Cohen, Gas Turbine Theory, 5th ed., Prentice Hall, Harlow, England, New York, 2001.
[37] R. Cirligeanu, V. Pachidis, Igv loss and deviation modelling (Master's thesis), Cranfield University, 2010.
[38] A. Howell, Fluid dynamics of axial compressors, Proc. Inst. Mech. Eng. 153 (1) (1945) 441–452.
[39] N. White, A. Tourlidakis, R. Elder, Axial compressor performance modelling with a quasi-one-dimensional approach, Proc. Inst. Mech. Eng. Part A 216 (2) (2002) 181–193.
[40] P. Wright, D. Miller, R.-R. Ltd, An Improved Compressor Performance Prediction Model, Rolls-Royce plc, 1991.
[41] F.C. Schwenk, G.W. Lewis, M.J. Hartmann, A preliminary analysis of the magnitude of shock losses in transonic compressors (Tech. rep.), NASA, 1957.
[42] W.M. Osborn, R.D. Moore, R.J. Steinke, Nasa, Aerodynamic performance of a 1.35-pressure-ratio axial-flow fan stage (NASA Technical Paper), Nasa, Washington, D.C., 1978.
[43] F. Berg, J. Palmer, P. Miller, M. Husband, G. Dodds, HTS electrical system for a distributed propulsion aircraft, IEEE Trans. Appl. Supercond. 25 (3) (2015).
[44] R. de Vries, M. Hoogreef, R. Vos, Aero-propulsive efficiency requirements for turboelectric transport aircraft, AIAA Scitech 2020 Forum, 2020.
[45] S.S. Kalsi, J. Storey, K. Hamilton, R.A. Badcock, Propulsion motor concepts for airplanes, AIAA Propulsion and Energy 2019 Forum, 2019.